GLIA

WILEY

RESEARCH ARTICLE

Oligodendrocytes regulate the adhesion molecule ICAM-1 in neuroinflammation

María Nazareth González-Alvarado[1] [iD] | Jessica Aprato[2] | Melissa Baumeister[1] |
Magdalena Lippert[1] | Arif B. Ekici[3] | Philipp Kirchner[3] | Tobias Welz[4] |
Alana Hoffmann[5] | Jürgen Winkler[5] | Michael Wegner[2] | Stefanie Haase[1] |
Ralf A. Linker[1,6]

[1]Department of Neurology, University Hospital Regensburg, Regensburg, Germany

[2]Department of Biochemistry, Friedrich-Alexander University Erlangen-Nuremberg (FAU), Erlangen, Germany

[3]Institute of Human Genetics, University Hospital Erlangen, Friedrich-Alexander University Erlangen-Nuremberg (FAU), Erlangen, Germany

[4]Department of Neurology and Molecular Cell Biology, University Hospital Regensburg, Regensburg, Germany

[5]Department of Molecular Neurology, University Hospital Erlangen, Friedrich-Alexander University Erlangen-Nuremberg (FAU), Erlangen, Germany

[6]Department of Neurology, University of Regensburg, Regensburg, Germany

Correspondence
Ralf A. Linker, Department of Neurology, University Hospital Regensburg, Germany.
Email: ralf.linker@klinik.uni-regensburg.de

Funding information
Deutsche Forschungsgemeinschaft, Grant/Award Number: 270949263/GRK2162

Abstract

Recently, oligodendrocytes (Ol) have been attributed potential immunomodulatory effects. Yet, the exact mode of interaction with pathogenic CNS infiltrating lymphocytes remains unclear. Here, we attempt to dissect mechanisms of Ol modulation during neuroinflammation and characterize the interaction of Ol with pathogenic T cells. RNA expression analysis revealed an upregulation of immune-modulatory genes and adhesion molecules (AMs), ICAM-1 and VCAM-1, in Ol when isolated from mice undergoing experimental autoimmune encephalomyelitis (EAE). To explore whether AMs are involved in the interaction of Ol with infiltrating T cells, we performed co-culture studies on mature Ol and Th1 cells. Live cell imaging analysis showed direct interaction between both cell types. Eighty percentage of Th1 cells created contacts with Ol that lasted longer than 15 min, which may be regarded as physiologically relevant. Exposure of Ol to Th1 cells or their supernatant resulted in a significant extension of Ol processes, and upregulation of AMs as well as other immunomodulatory genes. Our observations indicate that blocking of oligodendroglial ICAM-1 can reduce the number of Th1 cells initially contacting the Ol. These results suggest that AMs may play a role in the interaction between Ol and Th1 cells. We identified Ol interacting with CD4$^+$ cells in vivo in spinal cord tissue of EAE diseased mice indicating that our in vitro findings are of interest to further scientific research in this field. Further characterization and understanding of Ol interaction with infiltrating cells may lead to new therapeutic strategies enhancing Ol protection and remyelination potential. Oligodendrocytes regulate immune modulatory genes and adhesion molecules during autoimmune neuroinflammation Oligodendrocytes interact with Th1 cells in vitro in a physiologically relevant manner Adhesion molecules may be involved in Ol-Th1 cell interaction.

KEYWORDS

adhesion molecules, autoimmune neuroinflammation, EAE, oligodendrocytes, Th1 cells

1 | INTRODUCTION

Neuroinflammation is a complex response of the central nervous system (CNS) against injury, pathogens, misfolded proteins and agents that disturb CNS homeostasis. This response is mainly orchestrated by resident glial cells, although upon brain blood barrier (BBB) disruption, it may also involve the peripheral immune system. Neuroinflammation is a hallmark for many neurological diseases, but major infiltration of autoreactive lymphocytes is a pivotal feature of multiple sclerosis (MS). The autoimmune response in MS targets the myelin layer and results in characteristic demyelinating lesions, oligodendrocyte (Ol) death and eventually axonal damage as well as neuronal loss. The mechanisms that lead to antigen presentation and autoimmunity against myelin antigens are not completely understood. Yet, mounting evidence indicates that auto reactive CD4$^+$ T helper cells play an important role in the development of the disease (Kaskow & Baecher-Allan, 2018; Severson & Hafler, 2010; Traugott et al., 1982).

Currently, the exact mechanisms behind CD4$^+$ T cell induced Ol damage remain largely unclear (Antel et al., 1998; Zaguia et al., 2013). Evidence indicates that T cells may injure Ol via cell–cell contact, soluble factors or by modulating the inflammatory milieu (Kirby et al., 2019; Moore et al., 2015; Popko & Baerwald, 1999; Zaguia et al., 2013). Due to the high metabolic demands of myelin production, Ol are very sensitive to inflammation, thus they have been disregarded as active players in neuroinflammation (McTigue & Tripathi, 2008). However, recent studies are challenging this established concept and suggest that Ol may act as immunomodulators of their environment by expressing a variety of inflammation-related genes and perhaps even being able to interact with the peripheral immune system (Falcão et al., 2018; Jäkel et al., 2019; Kirby et al., 2019; Madsen et al., 2020; Satoh, Kim, et al., 1991).

Immune cells mainly communicate via chemokines and cytokines, polypeptides with the capacity to influence cell behavior. However, CD4$^+$ T cells also employ direct cell–cell contact for communication (Becher et al., 2000). The adhesion molecules (AMs) intracellular adhesion molecule 1 (ICAM-1) and vascular cell adhesion molecule 1 (VCAM-1) play a fundamental role in lymphocyte-endothelium interaction and T cell activation (Haghayegh et al., 2019; Steiner et al., 2010) and are upregulated in Ol in inflammatory conditions (Satoh, Kastrukoff, & Kim, 1991; Satoh, Kim, et al., 1991). Thus, they represent suitable candidates for mediating Ol interaction with infiltrating lymphocytes.

Here we explore the possibility that AMs may be involved in T cell-Ol interplay during autoimmune neuroinflammation. Our results support the novel concept of Ol developing an immune phenotype under certain inflammatory settings. Additionally, we describe a Th1 cell-Ol interaction in vitro and observe the formation of stable contacts that may be considered physiologically relevant. A Th1 cell related inflammatory environment exerts morphological changes on Ol and induces the expression of immune related genes as well as AMs, ICAM-1, and VCAM-1. Our data suggest that ICAM-1 may play a role in the interaction between Ol and Th1 cells.

2 | MATERIALS AND METHODS

2.1 | Mice strains and maintenance

C57BL/6J mice were initially purchased from Charles River breeding laboratories (Sulzfeld, Germany). All mice were housed at the central animal laboratory (ZTL), the animal care facility of the University Hospital in Regensburg (Germany) under a 12 h day/night cycle and standardized environmental conditions receiving normal or powder chow and tap water ad libitum. All mice strains bred in-house were backcrossed on a C57BL/6J background for at least 10 generations. All experiments were in accordance with the German laws for animal protection and were approved by the local ethic committees for animal welfare (55.22532-2-450/55.2-2532.2-395).

2.2 | Induction of active experimental autoimmune encephalomyelitis (EAE)

For active EAE induction, 10–15 weeks old mice, C57BL/6J were anesthetized with intraperitoneal (i.p.) injection of ketamin/xylazin. Mice were subcutaneously (s.c.) injected with 200 μg myelin oligodendrocyte glycoprotein (MOG)$_{35-55}$ or 200 μg of ovalbumin (OVA), together with 200 μg of complete Freund's adjuvant (CFA) containing 4 mg/ml Mycobacterium tuberculosis (H37Ra). Pertussis toxin (200 ng/mouse) was applied i.p. on days 0 and 2 post immunization (p.i.). Clinical symptoms were assessed daily according to a 10-point scale: 0: no symptoms; 1: reduced tone of the tail; 2: limp tail; 3: rolling gait; 4: ataxic gait; 5: mild paraparesis of hind limbs; 6: severe paraparesis; 7: complete paraplegia of hind limbs, 8: tetraparesis; 9: tetraparesis, respiratory distress, moribund; 10: death (Linker et al., 2002). Mice that exceeded a clinical score of 7 were killed in accordance with animal welfare. Animals were perfused via the left cardiac ventricle with 4% PFA solution. The CNS was removed and embedded either in paraffin or OCT cryo embedding matrix. For gene expression analysis, animals were perfused via the left cardiac ventricle with PBS and O4$^+$ cells were isolated from whole brain or spinal cord before RNA isolation and qPCR analysis. Extraction of tissue for the analysis of Ol-Th1 cell interaction in vivo was performed 4 days after the mice reached peak of disease.

2.3 | Cuprizone model

To induce full toxic demyelination of the corpus callosum (CC), 8–10 weeks old C57BL/6J mice were exposed to 0.2% cuprizone (Bis [cyclohexanone] oxaldihydrazone, C9012, Sigma, St. Louis, MO, USA) mixed in powder standard rodent chow for 5 weeks. During this time, mice were monitored for weight loss and trained in a rotor rod to assess motor coordination. For remyelination analysis, animals were returned to normal diet in fresh cages for 3 days. Finally, mice were sacrificed at point of maximum demyelination (week 5) and at early remyelination point (week 5.5) and the brain was extracted for Ol

isolation. Age-matched mice receiving normal powder chow were used as naïve cuprizone controls.

2.4 | Neonatal oligodendrocyte isolation and culture

The brains from wild type (WT) mice younger than postnatal day 7 (P7) were extracted under sterile conditions and kept in cold hank's balanced salt solution (HBSS) (without Ca^{2+} or Mg^{+2}) until dissociation according to the neural tissue disassociation kit protocol (130-092-628, Miltenyi, Bergisch Gladbach, Germany). $CD140^{+}$ cells were isolated using MACS magnetic columns following the anti-CD140 microbeads protocol (130-101-502, Miltenyi, Bergisch Gladbach, Germany). Briefly, magnetic labeled CD140 antibody binds to cells expressing the corresponding antigen. These cells are applied to a MACS column and retained in a strong magnetic field. The cells can be collected by removing the column from the magnetic field and pushing them out of the column. Labeled cells were plated on slides or plates pre-coated with poly-L-lysine (PLL) overnight at 37°C and kept in MACS neuro media (130-093-570, Miltenyi, Bergisch Gladbach, Germany) supplemented with 0.5 mM L-glutamine (G7513, Sigma, St. Louis, MO, USA), 10 ng/ml PDGF (130-108-983, Miltenyi, Bergisch Gladbach, Germany), 10 ng/ml FGF (130-105-786, Miltenyi, Bergisch Gladbach, Germany). To maintain the oligodendrocyte precursor cell (OPC) phenotype, half of the media was exchanged every day, cells were used after 2 days in vitro (DIV) for co-culture. For differentiation of OPC, the media was completely exchanged 24 h after plating for MACS neuro media, supplemented with 0.5 mM L-glutamine, 0.5% heat inactivated horse serum and 40 ng/ml 3′3,5-triiodo-L-thyronine (T3, Sigma, St. Louis, MO, USA), half of the media was exchanged every day for freshly prepared medium. Cells were used after 5 DIV for co-culture.

2.5 | T cell isolation and Th1 cell differentiation

The spleens of adult 2D2 mice were extracted under sterile conditions and conserved in cold HBSS (without Ca^{+2} or Mg^{+2}) until tissue disassociation. The spleen was triturated with a syringe plunge over a 70 μm filter, the filter was washed with RPMI 1640 media (Gibco, Darmstadt, Germany) and the solution was collected in a 50 ml falcon tube and centrifuged for 10 min, 300*g* at 4°C. After decanting the supernatant, the pellet was resuspended in 5 ml of NH_4Cl (0.14 M) and incubated for 10 min at room temperature (RT). The erythrocyte digestion was stopped with 20 ml of serum containing media, filtered with a 70 μm filter and centrifuged for 10 min, 300*g* at 4°C. The pellet was resuspended in 10 ml of PBS and the cell number was determined. $CD4^{+}$ naïve T cells were isolated using the naïve CD4 T cell isolation kit according to the manufacturer's instructions (130-104-453, Miltenyi, Bergisch Gladbach, Germany). After isolation, 100,000 cells were plated in a 96 well flat bottom plate pre-coated overnight with 2 μg/ml anti-CD3 (100,331, Biolegend, San Diego, CA, USA) at 4°C.

To keep T cells from differentiating (Th0), pre-absorbed anti-CD3 and soluble 2 μg/ml anti-CD28 (553,294, clone 37.51, BD Bioscience, Heidelberg, Germany) was used, in combination with 10 μg/ml anti-IFNγ (505,812, Biolegend, San Diego, CA, USA) and 10 μg/ml anti-IL-4 (554,432, BD Bioscience, Heidelberg, Germany) in re-stimulation media (Remed) (RPMI 1640 media supplemented with 10% [vol/vol] fetal calf serum, 1% penicillin/streptomycin, 1% nonessential amminoacids, 1% L-glutamine, 1% Na-pyruvate and 50 μM β-mercaptoethanol).

To induce a Th1 phenotype, in addition to pre-absorbed CD3, we added soluble 2 μg/ml anti-CD28 (553,294, clone 37.51, BD Bioscience, Heidelberg, Germany), 10 μg/ml anti-IL-4 (554,432, BD Bioscience, Heidelberg, Germany) and 0.02 μg/ml IL-12 (130-096-708, Miltenyi, Bergisch Gladbach, Germany) in Remed to the naïve T cells and kept them at 37°C for 3 days. Afterwards, half of the media was exchanged for RPMI media with 10% heat inactivated horse serum containing 20 U/ml IL-2 (130-098-221, Miltenyi, Bergisch Gladbach, Germany) and the cells were left to proliferate for 48 h.

2.6 | Co-culture of oligodendrocytes and Th1 cells

T cells were harvested, resuspended and counted. Next, they were centrifuged for 5 min at 300 g and resuspended to a density of 1×10^{6} cells/ml in co-culture media, 50% RPMI with 10% heat inactivated horse serum and 50% of proliferation media for OPC co-culture and differentiation media for Ol co-culture. The T cells were seeded with Ol at a ratio of 5:1, respectively, and cultured for 24 h at 37°C under constant 5% CO_2. After incubation, both cell types were collected separately for either FACS analysis, RNA analysis or immunofluorescence staining. The supernatant of Th1 cells was collected and added to Ol in a 1:1 proportion with proliferation (OPC) or differentiation (Ol) media for 24 h.

2.7 | Live cell imaging of co-culture experiments

For live cell imaging of the co-culture, Th1 or Th0 cells were added right before transport to the microscope, in addition of 20 mM Hepes. Cells were imaged for 1.5 h at 37°C, 5% humidity with an inverted Leica AF6000LX microscope, equipped with a Leica DFC350 FX digital camera (Leica, Wetzlar, Germany). Bright field images were taken every 5 min under a 10x objective, using the Leica LASX software. The images were exported as videos and analyzed with the ImageJ software using the cell counter plugin to determine the number of T cells in contact with Ol and Ol area. The number of Th1 cells in contact was normalized to the OPC/Ol area. The manual tracking plugin was used to follow the crawling behavior of the Th1 cells.

2.8 | Blocking experiments

To analyze the effect of blocking antibodies, 10 μg/ml anti-ICAM-1 antibody (14-0541-85, clone: YN1/1.7.4, Invitrogen, OR, USA) was added to the Ol and 10 μg/ml anti-VLA-4 (BE0071, clone: PS/2,

BioXcell, NH, USA) or 10 μg/ml anti-LFA-1 (555,280, clone: GAME-46, BD Pharmingen, CA, USA) to Th1 cells, 2 h before co-culture. The respective isotype was added to the control group. The blocking antibodies were kept at the same concentration throughout the 24 h co-culture.

2.9 | EdU assay

At the time of co-culture, 10 μM of EdU (C10340, Thermofisher, Waltham, MA, USA) was added to the media and left for 24 h at 37°C. After, the co-culture, cells were washed with PBS and fixed with a 3.7% PFA solution for 15 min at RT. After incubation, the PFA was removed and the cells were washed with 3% BSA/PBS and permeabilized with 0.5% triton-X in PBS for 20 min at RT. The permeabilization was removed and cells were washed twice with 3% BSA/PBS. The reaction cocktail was prepared according to the manufacturer's instructions, added to the cells and kept them in the dark for 30 min at RT. After the incubation, cells were washed with 3% BSA/PBS, block with 10% BSA/PBS for 1 h at RT. Subsequently, we incubated the cells with primary antibody rat CD140 1:75 (14-1401-82, Invitrogen, OR, USA) overnight at 4°C. Afterwards, the cells were washed and incubated with secondary antibody anti-rat Alexa-fluor 555 (A21434, Thermofisher, Waltham, MA, USA) for 1 h at RT, washed and imaged with an inverted Leica AF6000LX fluorescence microscope.

2.10 | Adult oligodendrocyte isolation

Adult Ol were isolated from whole brain or spinal cord. The tissue of adult mice was extracted and kept in cold HBSS (without Ca^{2+} or Mg^{2+}) until tissue disassociation. In brief, brains were dissociated in a gentle MACS Octo dissociator following the instructions provided by the adult brain dissociation kit (130-107-677, Miltenyi, Bergisch Gladbach, Germany). After dissociation, $O4^+$ cells were isolated using MACS magnetics columns following the anti-O4 microbeads protocol (130-094-543, Miltenyi, Bergisch Gladbach, Germany). The cells were preserved in BL buffer (Z6012, Promega, WI, USA) at −80°C until RNA isolation was performed or directly used in flow cytometry analysis.

2.11 | Immunohistochemistry

Mice were euthanized in a CO_2 chamber and perfused via the left cardiac ventricle with 4% PFA solution. The tissue was post fixated in PFA for 4 h and transferred to gradient of sucrose solutions 10, 20 and 30% sucrose for 24 h each. The spinal cord tissue was then cut transversally in cervical, thoracic and lumbar sections and embedded in O.C.T embedding medium and kept at −80°C until sectioning in a cryostat at −18°C in 6 μm sections. Prior to staining the slides were left to air dry at RT for minimum 1 h. Afterwards, they were fixed in acetone for 5 min at −20°C. After washing with PBS, the tissue sections were blocked with 10% BSA/0.2% Triton-X for 1 h at RT

and left with primary antibody rabbit Olig2 1:250 (AB9610, Millipore, Darmstadt, Germany) and rat ICAM-1 PE 1:100 (12–0541-81, Invitrogen, OR, USA) or rat CD4 FITC 1:100 (553,047, BD Bioscience, CA, USA) diluted in 1% BSA/PBS 0.2% Triton-X overnight at 4°C. Following washing steps, the slides were incubated with anti-rabbit Alexa-fluor 488 (A21425, Thermofisher, Waltham, MA, USA), anti-rat Alexa-fluor 555 (A21434, Thermofisher, Waltham, MA, USA), or anti-rabbit Alexa-fluor 647 (A21246, Thermofisher, Waltham, MA, USA) and anti-rat Alexa-fluor 488 (A11006, Thermofisher, Waltham, MA, USA) 1:1000 in 1% BSA/0.2% Triton-X for 45 min at RT in the dark. Finally, the sections were washed in PBS, incubated with DAPI for nuclear staining for 5 min at RT and mounted with antifade prolong reagent.

2.12 | Immunocytochemistry (ICC)

Ol were fixed with 4% PFA for 10 min. The cells were washed with PBS and blocked for 1 h with 10% BSA/0.1% between. Cells were incubated with primary antibodies, rabbit Nogo-A 1:750 (AB5888, Merck Millipore, Darmstadt, Germany), rat CD4 FITC 1:100 (553,047, BD Bioscience, CA, USA), at 4°C overnight. After washing steps with PBS-T, cells were incubated for 1 h with 1:1000 dilution of the corresponding secondary antibody anti-rabbit Alexa-fluor 647 (A21246, Thermofisher, Waltham, MA, USA) and anti-rat Alexa-fluor 488 (A11006, Thermofisher, Waltham, MA, USA). Nuclear staining was done by DAPI incubation for 5 min. Cells were mounted with antifade progold reagent and pictures were taken under a fluorescent Leica microscope. For phalloidin staining cells were fixed with 4% PFA for 10 min and permeabilized with 0.1% Triton-X in PBS for 5 min. After washing, they were incubated for 30 min at RT with 1% BSA/PBS, followed by a 20 min incubation with phalloidin 555 (A34055, Invitrogen, OR, USA) (1 unit) and nuclear staining was performed with DAPI. Cells were then washed and mounted.

2.13 | Microscopy and data analysis

Cell cultures were analyzed with an inverted Leica AF6000LX fluorescence microscope, equipped with a Leica DFC7000GT CCD camera (Leica, Wetzlar, Germany). Randomized pictures were taken with a Leica program from an eight or four well chamber slide with a Leica HC PL FLUOTAR L 20×/0.4 CORR PH1 objective. A blinded observer quantified positive cells from the digital images, using the plug-in cell counter from imageJ 1.52a (Rueden et al., 2017), and the area of Ol was determined with the same software. At least 300 cells were counted in three independent experiments per group. For quantification of MBP stained cells, cells were divided into simple, intermediate or complex cells. Cells were accounted as simple when they presented bipolar or tripolar morphology, intermediate cells possessed a more ramified structure but lacked membranous morphology present in complex cells, this quantification method was modified from Moore et al. (Moore et al., 2015).

To quantify ICAM-1 expression in Ol and Ol-CD4$^+$ T cell interaction in spinal cord, whole spinal cord sections were imaged with

FV3000 confocal microscope, with the 10 or 20× objective. The white matter area was defined in the ImageJ software and the cell counter plugin was used to identify double positive cells.

2.14 | Flow cytometry (FC)

Ol and Th1 cells were analyzed by staining of extra and intra-cellular markers. When intracellular cytokine staining was required, lymphocytes were stimulated with ionomycin (1 μM) and PMA (50 ng/ml) in the presence of monensin (2 μM) for 3 h at 37°C. First, dead cells were excluded by a fixable viability dye eFluor®780 (0.2 μl/test) for 20 min at 4°C in the dark. Following, cells were washed with PBS, nonspecific Fc-mediated interactions were blocked by addition of 0.5 μl αCD16/32 (FC block) (553,142, BD Bioscience, CA, USA) for 10 min at 4°C. For surface markers, T cells were stained with 1:200 dilution of the respective fluorochrome conjugated antibodies, CD4 FITC (553,047, BD Bioscience, CA, USA), VLA-4 PE (1:10, 130-102-555, Militeny, Bergisch Gladbach, Germany), LFA-1 PE (141,005, Biolegend, CA, USA) for 20 min in PBS. Oligodendrocytes were measured right after the 20 min incubation with O4 APC 1:50 (130-109-153, Militeny, Bergisch Gladbach, Germany), GalC FITC 1:25 (Fcamab3122F, Millipore, Darmstadt, Germany), ICAM-1 PE 1:80 (12-0541-81, Invitrogen, OR, USA), VCAM-1 FITC 1:50 (11-1061-82, Invitrogen, OR, USA) or VCAM-1 APC (17-1061-82 Invitrogen, OR, USA). To analyze the percentage of apoptotic cells in Ol population, cells were washed with binding buffer (51-6612E, BD Pharmingen, CA, USA) and incubated with Annexin V FITC (556,419, BD Pharmingen CA, USA) for 15 min at RT in the dark, after another wash with binding buffer, the cells were ready for measurement. For GFAP staining, cells were fixed with Fix/Perm buffer (00-5523-00, Life Technologies, Carlsbad, CA, USA) for 20 min at RT, washed and incubated with GFAP (130–118-351, Milteny, Bergisch Gladbach, Germany) for 10 min at RT, washed and measured. Lymphocytes were fixed with 1% PFA and made permeable with saponin buffer or Fix/Perm buffer (00-5523-00, Life Technologies, Carlsbad, CA, USA), according to the manufacturer's protocol. Intracellular cytokines were stained with 1:100 dilution of the respective fluorochrome conjugated antibodies, IFNγ APC (17-7311-82, Invitrogen, OR, USA) or TNFα APC (506,307, Biolegend, CA, USA) for 45–60 min at RT. Cells were measured with a flow cytometer (FACSCantoII) equipped with the Diva acquisition program and FACS data were analyzed using FlowJo software. The gating was established by using isotype and FMO (fluorescence minus one) controls.

2.15 | Real-time polymerase chain reaction (qPCR)

Gene expression was analyzed by real time PCR. Cells were lysed in BL buffer (Z6012, Promega, WI, USA) and kept at −80°C until RNA isolation. Total RNA was isolated using the ReliaPrep RNA Cell miniprep system (Z6012, Promega, WI, USA) following the manufacturer's instructions. RNA yield was quantified by absorbance measurements at 260 nm. Total RNA was used to reversely transcribe RNA into cDNA, using QuantiTect® transcriptase according to the protocols (205,310, QIAGEN,

Hilden, Germany). PCR reactions were performed at a 5 μl scale on a qTower 2.0 real time PCR System (Analytic Jena, Jena, Germany) in triplicates. Relative quantification was performed by the ΔΔCT method, normalizing target gene expression on β-Actin as housekeeping gene (Livak & Schmittgen, 2001).

2.16 | RNA sequencing

Ol were isolated as described from brain of EAE diseased mice. Total RNA from Ol was isolated using the ReliaPrep RNA miniprep system (Z6012, Promega, WI, USA) and RNA integrity was determined on a Bioanalyzer 2100 system (Agilent Technologies, CA, USA). Sequencing libraries were prepared from 100 ng RNA input material using the TruSeq Stranded mRNA kit (Illumina, CA, USA) according to the manufacturers' instruction and sequenced single end with 100 bp on a HiSeq2500 platform. TruSeq sequencing adapters are trimmed from the reads in Cutadapt (v1.18) (Martin, 2011) and reads with a length of less than 60 bp after trimming were discarded. Read quality was assessed before and after trimming with FastQC (v0.11.8). Trimmed reads were mapped to the mouse reference genome GRCm38 with the GENCODE annotation 23 using the splice-aware aligner STAR (v2.6.1c) (Dobin et al., 2013). Reads mapping to non-overlapping exons are counted and summarized as reads per gene using Subread FeatureCounts (v1.6.1) (Liao et al., 2014). Differential expression analysis between the two groups was performed on the count matrices using DESeq2 (v1.24.0) (Love et al., 2014) in R (v3.6.1) (R core Team, 2014). The resulting p-values were adjusted using the Benjamini and Hochberg approach for controlling the False Discovery Rate (FDR). Fold expression differences were shrunk using the apeglm method (Zhu et al., 2019). Genes with an adjusted p-value <0.05 were selected for input into the GOrilla system (Eden et al., 2009) for gene ontology analysis. The pathway analysis was done by using the STRING tool (Jensen et al., 2009). The RNA sequencing analysis was performed in collaboration with the Institute of Human Genetics, University Hospital Erlangen.

2.17 | Statistical analysis

Statistical analysis was performed using the GraphPad Prism software (GraphPad Software Inc., La Jolla, CA). All data were analyzed by one-way ANOVA followed by Tukey's post-test or Mann–Whitney U test. Data are presented as mean ± SEM; $^*p < .05$, $^{**}p < .01$, or $^{***}p < .001$ were considered to be statistically significant.

3 | RESULTS

3.1 | RNA sequencing analysis from brain derived Ol of EAE mice revealed regulation of immune related genes

RNA sequencing was performed in O4⁺ cells extracted from the brain of MOG-EAE mice at the peak of disease (mean clinical score = 5.5
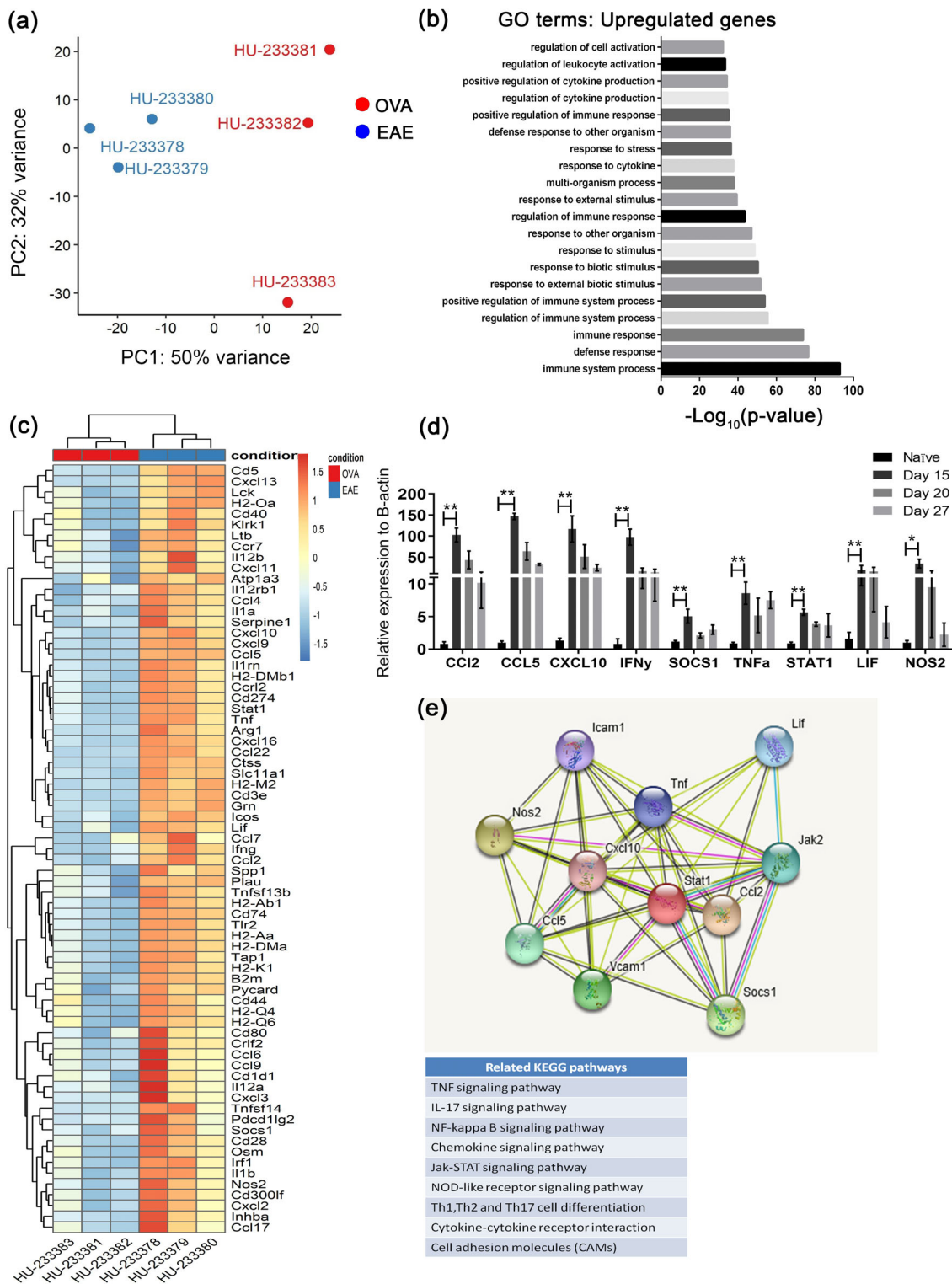
FIGURE 1 RNA sequencing from O4$^+$ cells isolated from the brain of OVA and MOG immunized mice. (a) Principal component analysis showed a clear segregation of the naïve and treated groups. (b) Gene ontology (GO) analysis depicts the 20 top functional categories of upregulated genes in the immunized group. (c) The heat map portrays the expression pattern of selected upregulated genes in the EAE group, belonging to immune related gene ontology categories. (d) Validation of selected genes via qPCR in OI during EAE disease course at day 15, 20, and 27 post immunization. (e) Pathway analysis shows that upregulated genes are involved in immune related mechanisms ($n = 3$ per group a–e)

± 1.3) (clinical course and individual scores are shown in Figure S1a,b) or ovalbumin immunized control mice. The purity of OI isolation is shown in Figure S2f. A principal component analysis revealed a clear segregation of both groups (Figure 1a) indicating differences in gene expression between both conditions. OI derived from MOG immunized mice significantly up-regulated 398 genes while significantly
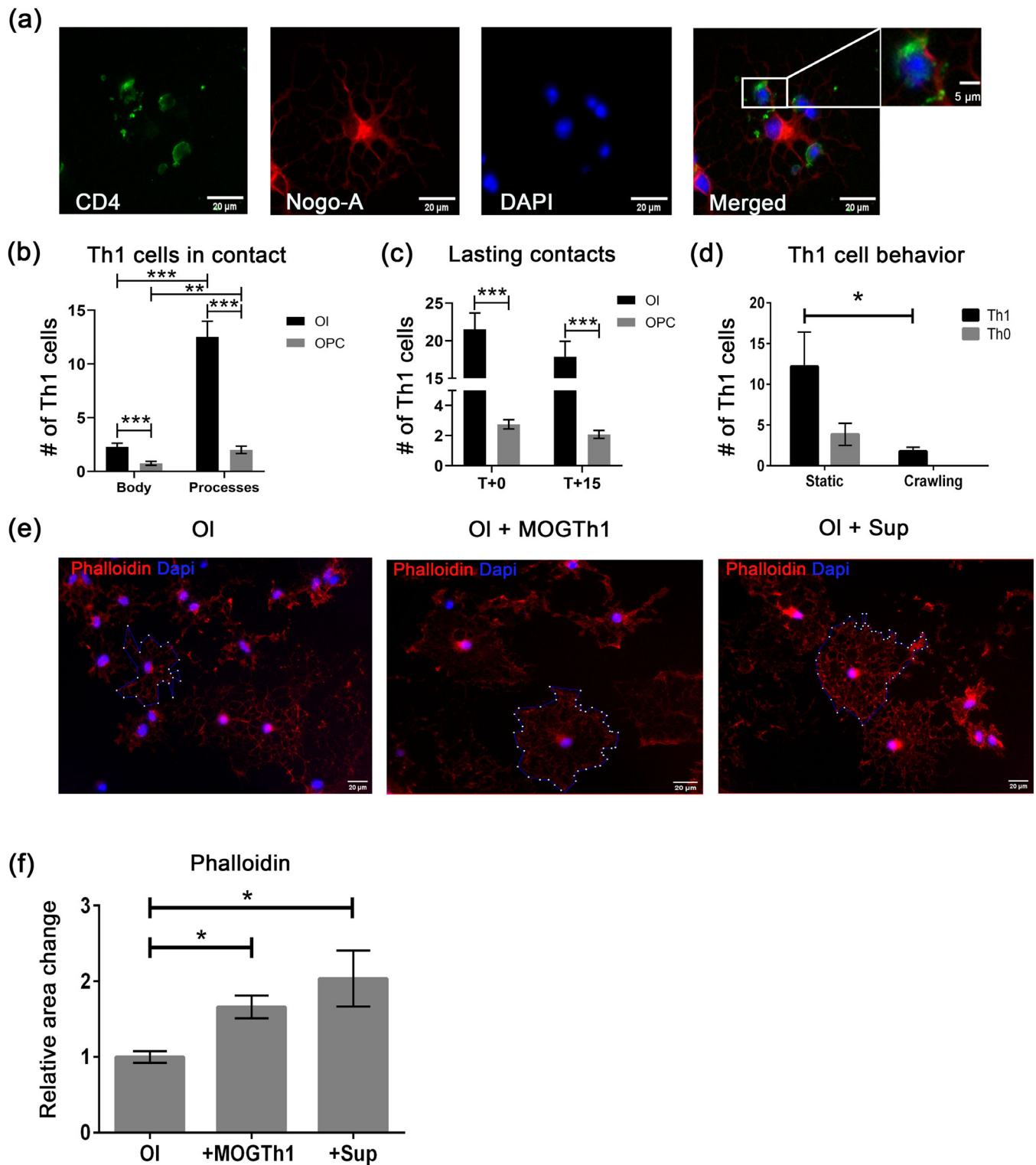
FIGURE 2 ICC and live cell imaging analysis of Th1 cell-Ol co-culture. (a) Representative images of Th1 cell-Ol interaction, after 24 h co-culture are shown; T cells were stained with CD4 (green), Ol with Nogo-A (red) and nuclear staining with DAPI (blue) (scale bar = 20 μm, scale bar in magnification = 5 μm). (b) Quantification of the live cell imaging displays the number of Th1 cells that contact the OPC/Ol body or processes, significantly less Th1 cells contacted OPC in comparison to Ol. (c) Analysis of Th1 cells establishing lasting contacts with OPC/Ol (d) Th1 cells presented either a static interaction with the Ol or a crawling behavior along Ol processes, Th0 cells did not present this crawling behavior (n = 3–4 independent experiments b–d). (e) Representative pictures of Ol alone and after co-culture with Th1 cells or supernatant; cells were stained with phalloidin (red) and DAPI (blue) (scale bar = 20 μm).) (f) After 24 h co-culture, Ol displayed changes in morphology analyzed by phalloidin staining (n = 3–4 independent experiments per group)

downregulating 126 genes (Tables S1 and S2) in comparison to the naïve group (Figure S1c). A gene ontology analysis revealed that most upregulated genes were involved in immune regulation processes and response to external stimuli (Figure 1b) whereas downregulated genes corresponded to a wider range of categories related to membrane transport and cell signaling (Table S1). Heatmap visualization highlighted differential expression of the upregulated genes, compared to the naïve group, inside the gene ontology category of "regulation of immune response" and involved in processes such as regulation of cell–cell adhesion, peptide binding and cytokine and chemokine activity (Figure 1c). All upregulated genes are also depicted in a heat map (Figure S1d). Additionally, we validated these results via qPCR analysis on Ol from the EAE model during disease progression (Figure 1d) (the clinical course and scores at time of euthanasia are shown in Figure S3f,g) and confirmed their significant upregulation at the peak of disease in comparison to Ol from aged matched naïve controls (mice without immunization, referred to as naïve in the figures). The genes depicted in the heat map were subjected to a pathway analysis. As expected, they are involved in many neuroinflammation-related signaling pathways (Figure 1e).

## 3.2 | Live cell imaging of MOGTh1 cell-Ol co-culture demonstrated the formation of stable contacts

Next, we implemented a co-culture with differentiated primary Ol and pro-inflammatory Th1 cells harboring a MOG specific T cell receptor (TCR; referred to as "Th1 cells") to explore how an inflammatory environment directly affects Ol. At the time of co-culture, the Ol expressed MOG both at the RNA and protein level (Figure S2a,b) and ~80% of the T cells were IFNγ positive (Figure S2c). In addition, we co-cultured Th1 cells with OPC. The OPC and Ol culture were characterized via ICC, showing a clear distinction between the cell types in each culture. OPC cultures were mainly composed of CD140$^+$ cells whereas the Ol culture mainly contained CNPase$^+$ cells and greatly reduced CD140 expression (Figure S2d,e). We performed live cell imaging of the co-culture to investigate the interaction between both cell types and observed that Th1 cells were able to form stable contacts with OPC and Ol, lasting longer than 15 min (Figure 2a,c). Mostly, Th1 cells attached to the Ol processes (Figure 2b) and a small percentage presented a crawling behavior along the Ol process (Figure 2d). This crawling behavior was unique to Th1 cells and was not observed with Th0 cells (Figure 2d), and was rarely observed in the OPC co-culture (data not shown). Interestingly, Ol experienced morphological changes during co-culture with Th1 cells. They significantly increased the coverage area of their processes, as evidenced by live cell imaging and quantified by phalloidin staining after 24 h of co-culture (Figure 2e,f). These changes were not related to an increase in differentiation as quantified by MBP staining and flow cytometry analysis of GalC positive cells (Figure S3a,b). We also did not detect a significant change in proliferation, as quantified by an EdU assay (Figure S3d). The number of apoptotic OPC or Ol were not significantly affected by the co-culture (Figure S3c). A selected group of genes from the RNA sequencing was validated in the co-culture
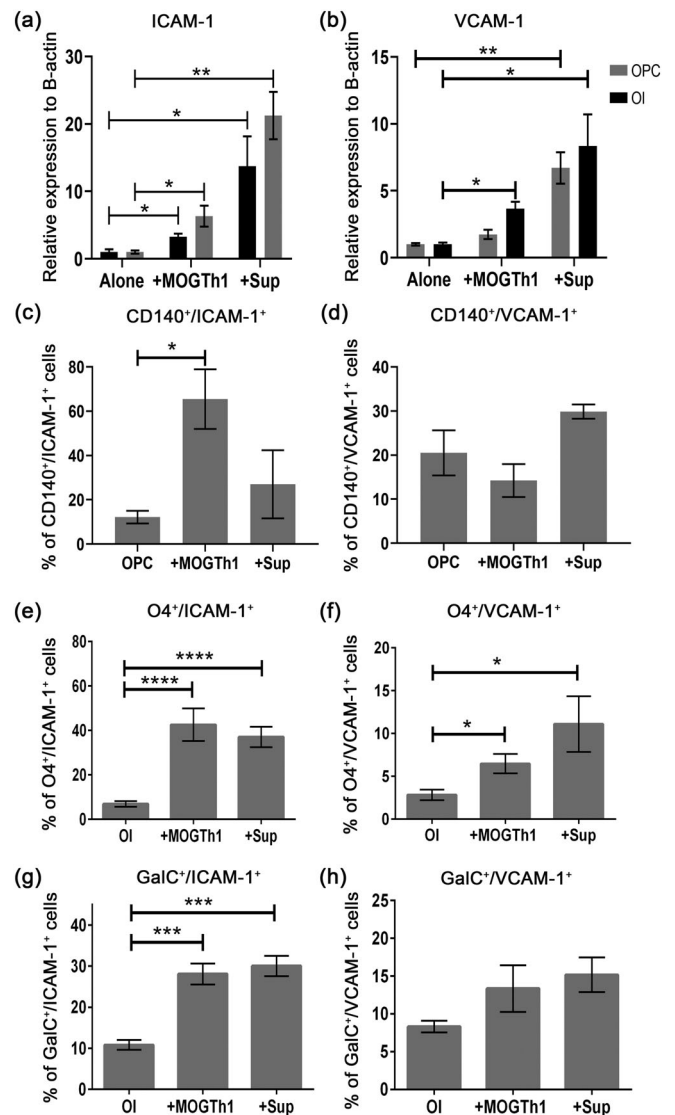
FIGURE 3   RNA and protein analysis of adhesion molecules in OPC and Ol after 24 h co-culture with Th1 cells. (a) OPC and Ol significantly upregulated RNA levels of ICAM-1 after co-culture with Th1 cells or their supernatant. (b) Ol upregulated RNA levels of VCAM-1 after co-culture and OPC upregulated VCAM-1 only in the presence of Th1 supernatant ($n = 4$ per group a–b). (c) Flow cytometry analysis of CD140$^+$ OPC after co-culture showed upregulation of ICAM-1 (d) but no change in VCAM-1. (e) Analysis of the early maturation marker O4 in the Ol-Th1 co-culture showed a significantly higher percentage of O4$^+$/ICAM-1$^+$ cells and (f) O4$^+$/VCAM-1$^+$ cells after co-culture. (g) In Ol-Th1 cell co-culture, quantification of the later maturation marker GalC, via FACS, showed a similar increase in percentage of GalC$^+$ cells co-expressing adhesion molecule ICAM-1 (h) but no significant changes in GalC$^+$/VCAM-1$^+$ cells ($n = 6$ per group c–f)

showing that Th1 related inflammatory milieu is sufficient to stimulate Ol to upregulate immune modulatory genes (Figure S3e). The upregulation of immune related genes in Ol may offer the possibility to modify their inflammatory environment. In consequence, we analyzed whether the co-culture had any significant effect on Th1 cells. After 24 h of co-culture
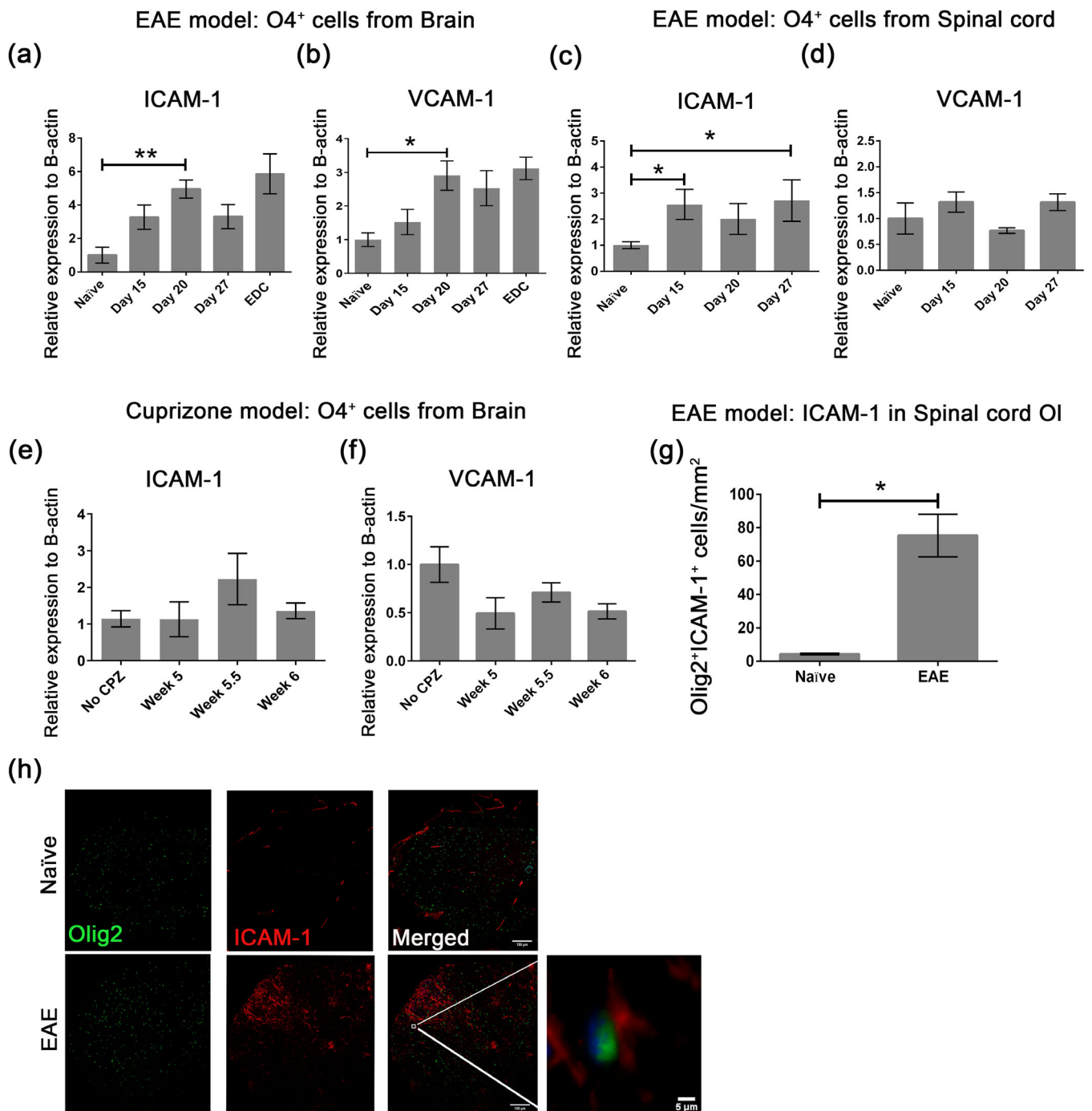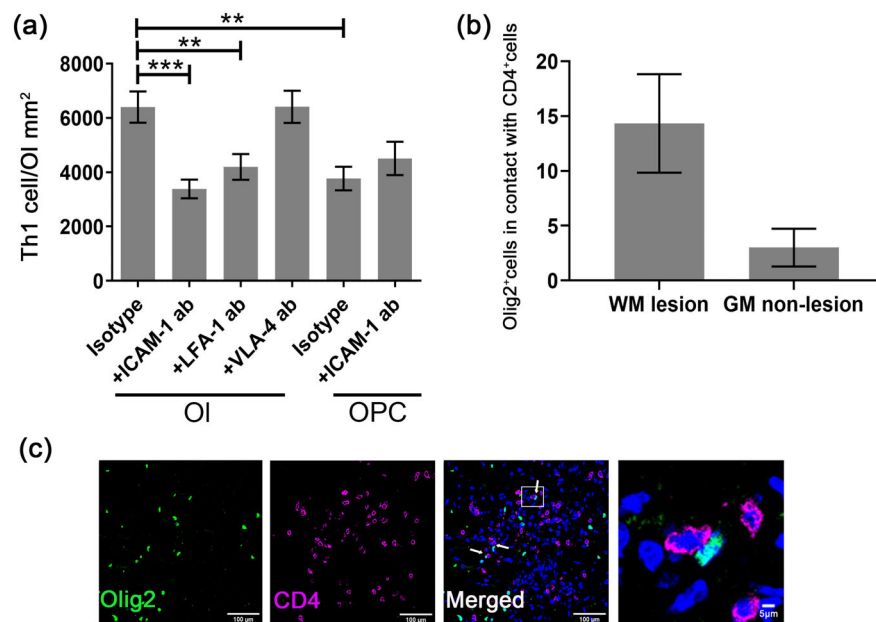
FIGURE 4 Analysis of adhesion molecule expression in Ol from in vivo models. (a) ICAM-1 RNA expression was significantly upregulated at day 20 of EAE in Ol extracted from the brain. (b) VCAM-1 RNA levels were significantly upregulated in Ol from brain of EAE diseased mice at day 20 p.i. (c) Ol isolated from spinal cord of MOG immunized mice showed significant upregulation of ICAM-1 at different stages of the disease. (d) VCAM-1 RNA levels remained unaltered during the course of EAE in Ol extracted from the spinal cord. (e) No changes in ICAM-1 expression were observed in Ol extracted from the brain of mice on a cuprizone diet. (f) No significant changes were observed in VCAM-1 RNA expression in Ol from the cuprizone model ($n = 3$–5 per group a–f). (g) Analysis of Olig2/ICAM-1 double positive cells showed a significant increase in Ol expressing the adhesion molecule ICAM-1 in the white matter of diseased mice ($n = 4$ per group). (h) Representative images of transversal spinal cord sections depicting Olig2$^+$ (green), ICAM-1$^+$ (red) and nuclear staining with DAPI (blue) (scale bar = 150 μm), a magnified 3D reconstruction showing an Ol expressing ICAM-1 (scale bar = 5 μm)

with mature Ol, Th1 cells downregulated the ICAM-1 receptor lymphocyte function associated antigen 1 (LFA-1) expression both at RNA and protein level and we observed a trend toward lower levels of pro-inflammatory cytokines IFNγ and TNFα (Figure S4a–h). Th1 cells exposed to OPC for 24 h did not show any significant changes in comparison to the control group (data not shown).

FIGURE 5 Effect of blocking antibodies against adhesion molecules in Th1 cell-Ol or OPC co-culture and immunofluorescence analysis of spinal cord from EAE diseased mice. (a) Blocking ICAM-1 on Ol significantly reduced the number of Th1 cells contacting Ol processes. A similar outcome was observed when blocking LFA-1 on Th1 cells, but no changes were seen by blocking VLA-4 on Th1 cells. Significantly less Th1 cells contacted OPC in comparison to mature Ol and blocking ICAM-1 had no effect in this interaction ($n = 3$–4 independent experiments). (b) Quantification of Olig2$^+$cells in contact with CD4$^+$cell in spinal cord of diseased mice showed that most interactions take place close to lesions but they also exist in the gray matter. (c) Representative pictures depicting the interaction between Olig2$^+$ (green) and CD4$^+$cells (magenta) in spinal cord, nuclear staining is shown by DAPI (blue). Interacting cells are pointed by the white arrows (scale bar $= 100$ μm) (scale bar in magnification $= 5$ μm) ($n = 3$)

3.3 | OPC and mature Ol upregulated adhesion molecules upon co-culture with MOGTh1 cells

To shed light on the mechanisms behind Th1 cell contact with Ol, we analyzed the expression of AMs in OPC and Ol after co-culture with Th1 cells or their supernatant. OPC and Ol per se showed only a very low expression of the AMs ICAM-1 and VCAM-1. After 24 h in the presence of Th1 cells, Ol significantly upregulated both AMs whereas OPC upregulated ICAM-1, but not VCAM-1 (Figure 3a,b). The inflammatory environment provided by the Th1 cell supernatant was sufficient to induce the observed upregulation of ICAM-1 and VCAM-1 in both OPC and Ol (Figure 3a,b). This upregulation of gene expression was mirrored by the analysis at the protein level as measured by flow cytometry of CD140$^+$ cells in the OPC culture and, O4$^+$ and GalC$^+$ cells in the mature Ol culture (Figure 3c–h). OPC did not upregulate VCAM-1 at the protein level (Figure 3d). More mature Ol, expressing the GalC marker, did not significantly upregulate expression of VCAM-1 (Figure 3f). Indicating that VCAM-1 may be quite specific to the pre-oligodendrocyte population expressing O4.

3.4 | Adhesion molecules were regulated in the EAE model but not in the cuprizone model

To identify the relevance of AMs expression in Ol in vivo, we employed the EAE and the cuprizone model in mice. We used O4$^+$

cells isolated from brain at different time points of cuprizone diet and O4$^+$ cells extracted from brain and spinal cord from MOG-EAE mice at different stages of the disease. RNA expression analysis showed that Ol upregulate the AMs ICAM-1 and VCAM-1 during EAE reaching higher expression levels at day 20 post-immunization in the brain (Figure 4a,b). In contrast, Ol isolated from spinal cord showed a more constant upregulation of ICAM-1 throughout the disease course and no significant upregulation of VCAM-1 (Figure 4c,d). Ol isolated from brain in the cuprizone model failed to show any significant regulation of these AMs (Figure 4e,f), suggesting that a particular inflammatory environment is necessary for inducing the upregulation of AMs in Ol and that the local inflammatory response linked to toxic demyelination is not sufficient to exert these changes. To further prove upregulation of ICAM-1 in Ol during EAE, analysis of immunofluorescence staining from spinal cord was performed in naïve versus diseased mice. The density of Olig2$^+$ cells expressing ICAM-1 significantly increased in the white matter of mice suffering from EAE symptoms (Figure 4g,h).

3.5 | Blocking oligodendroglial ICAM-1 reduced the number of contacts with Th1 cells

To understand the functional role of adhesion molecules in the Th1 cell-Ol interaction, we blocked ICAM-1 on Ol and OPC and LFA-1 or very late antigen 4 (VLA-4) on Th1 cells during the co-culture.

Quantification of the live cell imaging revealed that less Th1 cells contacted Ol processes when the ICAM-1 blocking antibody was present in culture (Figure 5a). A similar result was obtained when the corresponding integrin LFA-1 was blocked on Th1 cells (Figure 5a). Blockage of VLA-4 did not affect Th1 cells contacting Ol (Figure 5a). As compared to Ol, significantly less Th1 cells contacted OPC, and we observed no effect of blocking ICAM-1 on the number of Th1 cells contacting OPC (Figure 5a). ICAM-1 block did not interfere with the formation of stable contacts in OPC or Ol (Figure S5b). Th1 cell density did not vary between co-culture and crawling behavior was not altered by blocking antibodies (Figure S5a,c). Since the crawling behavior was rarely observed in the OPC co-culture, this was not further analyzed in the blocking experiments. In addition, we confirmed the interaction between Ol and T cell in vivo by staining spinal cord tissue of diseased mice (the clinical course and scores at the time of euthanasia are shown in Figure S3f,g). Quantification of Olig2$^+$ cells in contact with CD4$^+$ cells showed the presence of this interaction close to lesions but also, in much lower numbers, in the gray matter (Figure 5b,c).

4 | DISCUSSION

The metabolic demands of myelin production render Ol susceptible targets of neuroinflammation. Thus, Ol have been considered mere victims of inflammatory processes. Yet, OPC and Ol may be actively involved in immune modulatory processes, giving origin to the concept of inflammatory Ol (iOl) (Harrington et al., 2020). Consistently, our RNA sequencing analysis demonstrates that Ol from EAE diseased mice upregulated genes involved in antigen presentation, regulation of cytokine and chemokine production, response to IFNγ, cell–cell adhesion, among others. Falcão et al. (2018) described a similar regulation of immune related genes in Ol and OPC isolated from the spinal cord at the peak of EAE (Falcão et al., 2018). A similar immune phenotype has also been described in MS derived tissue samples (Jäkel et al., 2019). The potential of Ol to modulate the inflammatory milieu opens a new venue of research for therapeutic targets that may skew their immune modulatory capabilities to potentiate remyelination and survival during neuroinflammatory events.

We employed a co-culture system to analyze the impact of proinflammatory Th1 cells on OPC and mature Ol and to investigate possible interactions between these cell types. Here, we describe the formation of stable contacts between Th1 cells and Ol in vitro. Lasting significant interactions of T cells have been described to be longer than 10 min, implying that this contact has the potential to be physiologically relevant (Bartholomäus et al., 2009; Rezai-Zadeh et al., 2009). Previous studies have shown that OPC respond to injury rapidly and efficiently (Hampton et al., 2004; Levine & Reynolds, 1999; Rhodes et al., 2006). More recently, mature Ol have been implicated in such responses as well, showing that they may modulate immune related genes similarly to OPC, interact with proinflammatory cytokines and actively respond to injury (Balabanov et al., 2007; Knapp, 1997; Madsen et al., 2020). Moreover, a Th1 cell

inflammatory milieu resulted in morphological and transcriptional changes in mature Ol. Morphology changes in Ol as response to stress have been documented and thought to be relevant for remyelinating processes (Knapp, 1997; Pan et al., 2020). These findings emphasize the need to understand the effects of activated T cells in Ol subpopulations, as well as to reanalyze whether targeting specific inflammatory factors could prove more beneficial than complete blocking of T cell activation, a therapeutic approach currently used in certain neuroinflammatory conditions. Interestingly, we observed that mature Ol may have a slight modulatory effect on Th1 cells by inducing LFA-1 downregulation. After 24 h of co-culture, we did not find any particular effect of OPC in Th1 cells. Yet, Falcão et al. (2018) reported that co-culture of Th1 cells with OPC for 72 h resulted in a higher proliferation and number of cells producing IFNγ and TNFα (Falcão et al., 2018). Since mature Ol react differently than OPC to inflammatory conditions (Madsen et al., 2020), it could be expected that they also have distinct effects on the surrounding cells as suggested by our results.

ICAM-1 and VCAM-1 have a pivotal role in T cell activation and extravasation. Hence, they were considered as suitable candidates to facilitate the interaction with Ol. Ol exposed to Th1 cells and their supernatant or isolated from diseased EAE mice showed upregulation of both ICAM-1 and VCAM-1. In contrast, Ol from mice undergoing a cuprizone diet, hence exposed to a local glial response, did not regulate AMs, suggesting that the observed upregulation is linked to the presence of peripheral immune cells. Whether these AMs are involved in Th1 cell interaction with CNS resident cells is unknown. Blocking oligodendroglial ICAM-1 in a Th1 cell-Ol co-culture culminated in a reduced number of Th1 cells contacting the Ol processes. T cell studies have shown that ICAM-1/LFA-1 interaction displays a certain hierarchy over VCAM-1/VLA-4 when controlling T cell adhesion to the endothelium (Steiner et al., 2010). In the absence of ICAM-1, VCAM-1 served as an alternative ligand for T cells keeping a certain level of cell arrest and only blocking both molecules culminated in absolute T cell detachment (Bartholomäus et al., 2009; Steiner et al., 2010). Double blocking was not analyzed in the present work, opening the possibility that Th1 cells contacted Ol via alternative ligands such as ICAM-2 or 3, VCAM-1, and MHCII (Falcão et al., 2018; Miyamoto et al., 2016). Blocking ICAM-1 has resulted in ambiguous, possibly stage specific consequences, reporting both beneficial and detrimental outcomes in EAE (Archelos et al., 1993; Kawai et al., 1996; Willenborg et al., 1993). A few studies have characterized ICAM-1 expression in glial cells (Frohman et al., 1989; Sobel et al., 1990). However, Ol are rarely mentioned, emphasizing the need for further investigations on the role of ICAM-1 in oligodendroglial cells. Future studies should focus on oligodendroglia specific knockout of ICAM-1, rather than constitutive blockage, to study the specific effects that this molecule may have in myelinating glia and its interactions with infiltrating lymphocytes. We also reported the presence of Ol-T cell interaction in vivo, most cells in contact were found close to lesions but we also detected some in the gray matter. Recently, Ol-T cell interaction has been described in MS derived brain tissue (Larochelle et al., 2021). This

study also described Ol-Th17 cell interactions in mice that are MHCII independent, thus further strengthening a possible role of AMs in this interaction.

In conclusion, we observed a clear transcriptional remodeling in Ol in the context of the EAE model or when exposed to a Th1 cell related inflammatory milieu, endorsing the novel concept of iOl. Ol may possess inherent tools to modulate the detrimental inflammatory environment. Yet, to what extent they are actually able to favorably change inflammatory conditions remains unknown. Further research may shed light on how to boost the Ol immune response to favor remyelination. Pan et al. described that Ol previously infected with Mouse Hepatitis Virus remain immunologically active for up to 150 days post infection indicating that Ol may retain their immuno-competence long after the insult has disappeared (Pan et al., 2020). Additional studies on chronic EAE may offer some insights whether this is the case in autoimmune diseases as well. Finally, we report the formation of stable contacts between Th1 cells and Ol in vitro, which may be regulated to some extent by ICAM-1. AMs have long been therapeutic targets in autoimmunity. However, the approved drugs efalizumab and natalizumab, were either restricted from the market or bear some limitations due to a higher risk of progressive multifocal leukoencephalopathy (Seminara & Gelfand, 2010). The ICAM-1 blocker, enlimomab, resulted in higher mortality in stroke patients and only transient improvement in rheumatoid arthritis patients (Enlimomab Acute Stroke Trial, 2001; Kavanaugh et al., 1997). The present study emphasizes that besides the present caveats of thera-pies targeting integrins, AMs may also be involved in CNS system pro-cesses such as Ol responses to inflammation and interaction with peripheral immune cells. A better understanding of Ol behavior during inflammation and their interaction with infiltrating cells may help to skew their behavior toward beneficial outcomes thus improving the development of therapeutics halting the progression of autoimmune inflammatory CNS diseases.

CONFLICT OF INTEREST

The authors declare no conflict of interest.

DATA AVAILABILITY STATEMENT

The data that support the findings of this study are available from the corresponding author upon reasonable request. The data that support the findings of the RNA sequencing in this study are openly available in GEO (Gene Expression Omnibus) at https://www.ncbi.nlm.nih.gov/geo/, reference number GSE182341.

ORCID

María Nazareth González-Alvarado https://orcid.org/0000-0002-8799-7821

REFERENCES

Antel, J. P., McCrea, E., Ladiwala, U., Qin, Y. F., & Becher, B. (1998). Non-MHC-restricted cell-mediated lysis of human oligodendrocytes in vitro: Relation with CD56 expression. _Journal of Immunology_, _160_(4), 1606–1611.

Archelos, J. J., Jung, S., Mäurer, M., Schmied, M., Lassmann, H., Tamatani, T., Miyasaka, M., Toyka, K. V., & Hartung, H. P. (1993). Inhi-bition of experimental autoimmune encephalomyelitis by an antibody to the intercellular adhesion molecule ICAM-1. _Annals of Neurology_, _34_(2), 145–154. https://doi.org/10.1002/ana.410340209

Balabanov, R., Strand, K., Goswami, R., McMahon, E., Begolka, W., Miller, S. D., & Popko, B. (2007). Interferon—Oligodendrocyte interac-tions in the regulation of experimental autoimmune encephalomyelitis. _The Journal of Neuroscience_, _27_(8), 2013–2024. https://doi.org/10.1523/JNEUROSCI.4689-06.2007

Bartholomäus, I., Kawakami, N., Odoardi, F., Schläger, C., Miljkovic, D., Ellwart, J. W., Klinkert, W. E., Flügel-Koch, C., Issekutz, T. B., Wekerle, H., & Flügel, A. (2009). Effector T cell interactions with men-ingeal vascular structures in nascent autoimmune CNS lesions. _Nature_, _462_(7269), 94–98. https://doi.org/10.1038/nature08478

Becher, B., Prat, A., & Antel, J. P. (2000). Brain-immune connection: Immuno-regulatory properties of CNS-resident cells. _GLIA_, _29_(4), 293–304.

Dobin, A., Davis, C. A., Schlesinger, F., Drenkow, J., Zaleski, C., Jha, S., Batut, P., Chaisson, M., & Gingeras, T. R. (2013). Star: Ultrafast univer-sal RNA-seq aligner. _Bioinformatics (Oxford, England)_, _29_(1), 15–21. https://doi.org/10.1093/bioinformatics/bts635

Eden, E., Navon, R., Steinfeld, I., Lipson, D., & Yakhini, Z. (2009). Gorilla: A tool for discovery and visualization of enriched GO terms in ranked gene lists. _BMC Bioinformatics_, _10_, 48. https://doi.org/10.1186/1471-2105-10-48

Enlimomab Acute Stroke Trial. (2001). Use of anti-ICAM-1 therapy in ischemic stroke: Results of the Enlimomab acute stroke trial. _Neurol-ogy_, _57_(8), 1428–1434. https://doi.org/10.1212/wnl.57.8.1428

Falcão, A. M., van Bruggen, D., Marques, S., Meijer, M., Jäkel, S., Agirre, E., Samudyata, Floriddia, E. M., Vanichkina, D. P., Ffrench-Constant, C., Williams, A., Guerreiro-Cacais, A. O., & Castelo-Branco, G. (2018). Dis-ease-specific oligodendrocyte lineage cells arise in multiple sclerosis. _Nature Medicine_, _24_(12), 1837–1844. https://doi.org/10.1038/s41591-018-0236-y

Frohman, E. M., Frohman, T. C., Dustin, M. L., Vayuvegula, B., Choi, B., Gupta, A., … Gupta, S. (1989). The induction of intercellular adhesion molecule 1 (ICAM-1) expression on human fetal astrocytes by interferon-λ, tumor necrosis factor α, lymphotoxin, and interleukin-1: Relevance to intracerebral antigen presentation. _Journal of Neu-roimmunology_, _23_(2), 117–124. https://doi.org/10.1016/0165-5728(89)90030-1

Haghayegh-Jahromi N., Marchetti, L., Moalli, F., Duc, D., Basso, C., Tardent, H., Kaba, E., Deutsch, U., Pot, C., Sallusto, F., Stein, J. V., & Engelhardt, B. (2019). Intercellular adhesion Molecule-1 (ICAM-1) and ICAM-2 differentially contribute to peripheral activation and CNS entry of autoaggressive Th1 and Th17 cells in experimental autoimmune encephalomyelitis. *Frontiers in Immunology*, 10, 3056. https://doi.org/10.3389/fimmu.2019.03056

Hampton, D. W., Rhodes, K. E., Zhao, C., Franklin, R. J. M., & Fawcett, J. W. (2004). The responses of oligodendrocyte precursor cells, astrocytes and microglia to a cortical stab injury, in the brain. *Neuroscience*, 127(4), 813–820. https://doi.org/10.1016/j.neuroscience.2004.05.028

Harrington, E. P., Bergles, D. E., & Calabresi, P. A. (2020). Immune cell modulation of oligodendrocyte lineage cells. *Neuroscience Letters*, 715, 134601. https://doi.org/10.1016/j.neulet.2019.134601

Jäkel, S., Agirre, E., Mendanha Falcão, A., van Bruggen, D., Lee, K. W., Knuesel, I., Malhotra, D., Ffrench-Constant, C., Williams, A., & Castelo-Branco, G. (2019). Altered human oligodendrocyte heterogeneity in multiple sclerosis. *Nature*, 566(7745), 543–547. https://doi.org/10.1038/s41586-019-0903-2

Jensen, L. J., Kuhn, M., Stark, M., Chaffron, S., Creevey, C., Muller, J., Doerks, T., Julien, P., Roth, A., Simonovic, M., Bork, P., & von Mering, C. (2009). String 8—A global view on proteins and their functional interactions in 630 organisms. *Nucleic Acids Research*, 37(Database issue), D412–D416. https://doi.org/10.1093/nar/gkn760

Kaskow, B. J., & Baecher-Allan, C. (2018). Effector T cells in multiple sclerosis. *Cold Spring Harbor Perspectives in Medicine*, 8(4), a029025. https://doi.org/10.1101/cshperspect.a029025

Kavanaugh, A. F., Schulze-Koops, H., Davis, L. S., & Lipsky, P. E. (1997). Repeat treatment of rheumatoid arthritis patients with a murine anti-intercellular adhesion molecule 1 monoclonal antibody. *Arthritis and Rheumatism*, 40(5), 849–853. https://doi.org/10.1002/art.1780400511

Kawai, K., Kobayashi, Y., Shiratori, M., Sobue, G., Tamatani, T., Miyasaka, M., & Yoshikai, Y. (1996). Intrathecal administration of antibodies against LFA-1 and against ICAM-1 suppresses experimental allergic encephalomyelitis in rats. *Cellular Immunology*, 171(2), 262–268. https://doi.org/10.1006/cimm.1996.0202

Kirby, L., Jin, J., Cardona, J. G., Smith, M. D., Martin, K. A., Wang, J., Strasburger, H., Herbst, L., Alexis, M., Karnell, J., Davidson, T., Dutta, R., Goverman, J., Bergles, D., & Calabresi, P. A. (2019). Oligodendrocyte precursor cells present antigen and are cytotoxic targets in inflammatory demyelination. *Nature Communications*, 10(1), 3887. https://doi.org/10.1038/s41467-019-11638-3

Knapp, P. E. (1997). Injury stimulates outgrowth and motility of oligodendrocytes grown in vitro. *Experimental Cell Research*, 234(1), 7–17. https://doi.org/10.1006/excr.1997.3578

Larochelle, C., Wasser, B., Jamann, H., Löffel, J. T., Cui, Q.-L., Tastet, O., Schillner, M., Luchtman, D., Birkenstock, J., Stroh, A., Bittner, S., & Zipp, F. (2021). Pro-inflammatory T helper 17 directly harms oligodendrocytes in neuroinflammation. *Proceedings of the National Academy of Sciences of the United States of America*, 118(34). e2025813118. https://doi.org/10.1073/pnas.2025813118

Levine, J. M., & Reynolds, R. (1999). Activation and proliferation of endogenous Oligodendrocyte precursor cells during Ethidium bromide-induced demyelination. *Experimental Neurology*, 160(2), 333–347. https://doi.org/10.1006/exnr.1999.7224

Liao, Y., Smyth, G. K., & Shi, W. (2014). Featurecounts: An efficient general purpose program for assigning sequence reads to genomic features. *Bioinformatics (Oxford, England)*, 30(7), 923–930. https://doi.org/10.1093/bioinformatics/btt656

Linker, R. A., Mäurer, M., Gaup, S., Martini, R., Holtmann, B., Giess, R., Rieckmann, P., Lassmann, H., Toyka, K., Sendtner, M., & Gold, R. (2002). CNTF is a major protective factor in demyelinating CNS disease: A neurotrophic cytokine as modulator in neuroinflammation. *Nature Medicine*, 8(6), 620–624.

Livak, K. J., & Schmittgen, T. D. (2001). Analysis of relative gene expression data using real-time quantitative PCR and the 2(-Delta Delta C [T]) method. *Methods (San Diego, Calif.)*, 25(4), 402–408. https://doi.org/10.1006/meth.2001.1262

Love, M. I., Huber, W., & Anders, S. (2014). Moderated estimation of fold change and dispersion for RNA-seq data with DESeq2. *Genome Biology*, 15(12), 550. https://doi.org/10.1186/s13059-014-0550-8

Madsen, P. M., Desu, H. L., Rivero Vaccari, J. P., de Florimon, Y., Ellman, D. G., Keane, R. W., Clausen, B., Lambertsen, K. L., & Brambilla, R. (2020). Oligodendrocytes modulate the immune-inflammatory response in EAE via TNFR2 signaling. *Brain, Behavior, and Immunity*, 84, 132–146. https://doi.org/10.1016/j.bbi.2019.11.017

Martin, M. (2011). Cutadapt removes adapter sequences from high-throughput sequencing reads. *EMBnet. Journal*, 17(1), 10. https://doi.org/10.14806/ej.17.1.200

McTigue, D. M., & Tripathi, R. B. (2008). The life, death, and replacement of oligodendrocytes in the adult CNS. *Journal of Neurochemistry*, 107(1), 1–19. https://doi.org/10.1111/j.1471-4159.2008.05570.x

Miyamoto, Y., Torii, T., Tanoue, A., & Yamauchi, J. (2016). Vcam1 acts in parallel with CD69 and is required for the initiation of oligodendrocyte myelination. *Nature Communications*, 7, 13478. https://doi.org/10.1038/ncomms13478

Moore, C. S., Cui, Q.-L., Warsi, N. M., Durafourt, B. A., Zorko, N., Owen, D. R., Antel, J. P., & Bar-Or, A. (2015). Direct and indirect effects of immune and central nervous system-resident cells on human oligodendrocyte progenitor cell differentiation. *Journal of Immunology (Baltimore, MD: 1950)*, 194(2), 761–772. https://doi.org/10.4049/jimmunol.1401156

Pan, R., Zhang, Q., Anthony, S. M., Zhou, Y., Zou, X., Cassell, M., & Perlman, S. (2020). Oligodendrocytes that survive acute coronavirus infection induce prolonged inflammatory responses in the CNS. *Proceedings of the National Academy of Sciences of the United States of America*, 117(27), 15902–15910. https://doi.org/10.1073/pnas.2003432117

Popko, B., & Baerwald, K. D. (1999). Oligodendroglial response to the immune cytokine interferon gamma. *Neurochemical Research*, 24(2), 331–338. https://doi.org/10.1023/a:1022586726510

R core Team. (2014). *R (version v3.6.1) [computer software]*. R Foundation for Statistical Computing. http://www.R-project.org/

Rezai-Zadeh, K., Gate, D., & Town, T. (2009). Cns infiltration of peripheral immune cells: D-day for neurodegenerative disease? *Journal of Neuroimmune Pharmacology: The Official Journal of the Society on NeuroImmune Pharmacology*, 4(4), 462–475. https://doi.org/10.1007/s11481-009-9166-2

Rhodes, K. E., Raivich, G., & Fawcett, J. W. (2006). The injury response of oligodendrocyte precursor cells is induced by platelets, macrophages and inflammation-associated cytokines. *Neuroscience*, 140(1), 87–100. https://doi.org/10.1016/j.neuroscience.2006.01.055

Rueden, C. T., Schindelin, J., Hiner, M. C., DeZonia, B. E., Walter, A. E., Arena, E. T., & Eliceiri, K. W. (2017). Imagej2: Imagej for the next generation of scientific image data. *BMC Bioinformatics*, 18(1), 529. https://doi.org/10.1186/s12859-017-1934-z

Satoh, J., Kastrukoff, L. F., & Kim, S. U. (1991). Cytokine-induced expression of intercellular adhesion molecule-1 (ICAM-1) in cultured human oligodendrocytes and astrocytes. *Journal of Neuropathology and Experimental Neurology*, 50(3), 215–226. https://doi.org/10.1097/00005072-199105000-00004

Satoh, J., Kim, S. U., Kastrukoff, L. F., & Takei, F. (1991). Expression and induction of intercellular adhesion molecules (ICAMs) and major histocompatibility complex (MHC) antigens on cultured murine oligodendrocytes and astrocytes. *Journal of Neuroscience Research*, 29(1), 1–12. https://doi.org/10.1002/jnr.490290102

Seminara, N. M., & Gelfand, J. M. (2010). Assessing long-term drug safety: Lessons (re) learned from raptiva. *Seminars in Cutaneous Medicine and Surgery*, *29*(1), 16–19. https://doi.org/10.1016/j.sder.2010.01.001

Severson, C., & Hafler, D. A. (2010). T-cells in multiple sclerosis. *Results and Problems in Cell Differentiation*, *51*, 75–98. https://doi.org/10.1007/400_2009_12

Sobel, R. A., Mitchell, M. E., & Fondren, G. (1990). Intercellular adhesion molecule-1 (ICAM-1) in cellular immune reactions in the human central nervous system. *The American Journal of Pathology*, *136*(6), 1309–1316.

Steiner, O., Coisne, C., Cecchelli, R., Boscacci, R., Deutsch, U., Engelhardt, B., & Lyck, R. (2010). Differential roles for endothelial ICAM-1, ICAM-2, and VCAM-1 in shear-resistant T cell arrest, polarization, and directed crawling on blood–brain barrier endothelium. *The Journal of Immunology*, *185*(8), 4846–4855. https://doi.org/10.4049/jimmunol.0903732

Traugott, U., Scheinberg, L. C., & Raine, C. S. (1982). Multiple sclerosis: Heterology among early T cells and Tg cells. *Annals of Neurology*, *11*(2), 182–186. https://doi.org/10.1002/ana.410110212

Willenborg, D. O., Simmons, R. D., Tamatani, T., & Miyasaka, M. (1993). ICAM-1-dependent pathway is not critically involved in the inflammatory process of autoimmune encephalomyelitis or in cytokine-induced inflammation of the central nervous system. *Journal of Neuroimmunology*, *45*(1–2), 147–154. https://doi.org/10.1016/0165-5728(93)90175-X

Zaguia, F.Saikali P., Ludwin, S., Newcombe, J., Beauseigle, D., McCrea, E., Duquette, P., Prat, A., Antel, J. P., & Arbour, N. (2013). Cytotoxic NKG2C+ CD4 T cells target oligodendrocytes in multiple sclerosis. *Journal of Immunology (Baltimore, MD.: 1950)*, *190*(6), 2510–2518. https://doi.org/10.4049/jimmunol.1202725

Zhu, A., Ibrahim, J. G., & Love, M. I. (2019). Heavy-tailed prior distributions for sequence count data: Removing the noise and preserving large differences. *Bioinformatics (Oxford, England)*, *35*(12), 2084–2092. https://doi.org/10.1093/bioinformatics/bty895

SUPPORTING INFORMATION

Additional supporting information may be found in the online version of the article at the publisher's website.